Genomic programming of IRF4-expressing human Langerhans cells

Sofia Sirvent (1), Andres F. Vallejo (1), James Davies (1), Kalum Clayton (1), Zhiguo Wu (2), Jeongmin Woo (3), Jeremy Riddell (4), Virendra K. Chaudhri[#] (2), Patrick Stumpf (5), Liliya Angelova Nazlamova (1), Gabrielle Wheway (5), Matthew Rose-Zerilli (6), Jonathan West (6,7), Mario Pujato (8), Xiaoting Chen (4), Christopher H. Woelk (9), Ben MacArthur (6,7), Michael Ardern-Jones (1), Peter S Friedmann (1), Matthew T. Weirauch (4, 10), Harinder Singh*[#] (2, 10), Marta E Polak* (1, 7)

1. Clinical and Experimental Sciences, Sir Henry Wellcome Laboratories, Faculty of Medicine, University of Southampton, SO16 6YD, Southampton, UK
2. Division of Immunobiology & Center for Systems Immunology, Cincinnati Children's Hospital Medical Center, Cincinnati, OH, 45229, USA
3. Samsung Genome Institute, Samsung Medical Center, Seoul, South Korea
4. Center for Autoimmune Genomics and Etiology, Cincinnati Children's Hospital Medical Center, Cincinnati, OH, 45229, USA
5. Human Development and Health, Faculty of Medicine, University of Southampton, Southampton SO17 1BJ, UK
6. Cancer Sciences, Faculty of Medicine, University of Southampton, SO16 6YD, Southampton, UK
7. Institute for Life Sciences, University of Southampton, SO17 1BJ, UK.
8. Division of Biomedical Informatics, Cincinnati Children's Hospital Medical Center, Cincinnati, OH, 45229, USA
9. Merck's Exploratory Science Center, Cambridge, MA 02141, USA.
10. Department of Pediatrics, University of Cincinnati College of Medicine, Cincinnati, Ohio, 45229, USA

[#]Current address: Center for Systems Immunology, Departments of Immunology and Computational and Systems Biology, The University of Pittsburgh, Pittsburgh, PA 15213

Key words: Langerhans cells, Human skin, transcriptional and chromatin profiling, antigen presentation, IRF4 mediated programming, scRNA-seq, CRISPR editing

Abstract

Langerhans cells (LC) can prime tolerogenic as well as immunogenic responses in skin, but the genomic states and transcription factors (TFs) regulating these context-specific responses are unclear. Bulk and single-cell transcriptional profiling demonstrates that human migratory LCs are robustly programmed for MHC-I and MHC-II antigen presentation. Chromatin analysis reveals enrichment of ETS-IRF and AP1-IRF composite regulatory elements in antigen-presentation genes, coinciding with expression of the TFs, PU.1, IRF4 and BATF3 but not IRF8. Migration of LCs from the epidermis is accompanied by upregulation of IRF4, antigen processing components and co-stimulatory molecules. TNF stimulation augments LC cross-presentation while attenuating IRF4 expression. CRISPR-mediated editing reveals IRF4 to positively regulate the LC activation program, but repress NF2EL2 and NF-kB pathway genes that promote responsiveness to oxidative stress and inflammatory cytokines. Thus, IRF4-dependent genomic programming of human migratory LCs appears to enable LC maturation while attenuating excessive inflammatory and immunogenic responses in the epidermis.

Introduction

Langerhans cells (LCs) reside in the epidermis as a dense network of immune system sentinels. They are uniquely specialised at sensing the environment by extending dendrites through inter-cellular tight junctions to gain access to the *stratum corneum*, the outermost part of the skin. LC are highly specialised antigen presenting cells, priming protective immune responses against pathogens encountered via the skin, such as viruses[1-3], bacteria[4] and fungi [5]. They also promote responses to chemical sensitizers[6,7]. Their position in the outermost layers of the skin barrier and their capacity to sense dangerous perturbations to their environment make them a critical first line of defence in the skin. LCs also appear to play a vital role in maintaining immune homeostasis in the skin by activating skin resident memory T regulatory cells [5]. In the context of foreign pathogens LCs more effectively induce activation and proliferation of skin resident effector memory T cells and dampen memory T regulatory cell responses. Thus, it is important to elucidate regulatory pathways and mechanisms in LCs that enable their context-dependent functions in promoting tolerogenic as well as immunogenic responses in the epidermis.

LCs are highly efficient at presenting exogenous antigens in the context of MHC Class II thereby priming antigen-specific CD4 T cells [8]. Such responses include the activation of naïve CD4 T cells in skin draining lymph nodes as well as resident memory CD4 T cells in the skin [5]. LCs are also capable of efficient cross-presentation in which exogenous antigens are presented on MHC class I, resulting in activation and expansion of antigen-specific effector CD8 T cells[2,5,9,10]. Such cross-presentation becomes particularly important for adaptive immune responses against viruses and also cancerous cells which have evolved immune evasion mechanisms that inactivate DCs [11,12].

Activation of skin immune responses requires participation of epidermal cells in collaboration with LCs; cross-talk between the epidermal and immune components being critical. For example, in models of cutaneous viral infection, including vaccinia virus, only skin structural cells support virus replication, while immune cells, including LCs, are infected abortively [13], necessitating antigen transfer between epithelial and immune cells. Cytokine signalling from keratinocytes impacts LC development and function. Epidermal TGF-β and BMP7 are required for LC development and tolerogenic function *in vitro* [14-16] and cytokine signalling via thymic stromal lymphopoietin (TSLP) in atopic skin disease polarises skin dendritic cells to prime Th2 and Th22 CD4 T cell responses, while reducing the ability of LCs

to cross-prime CD8 T cells [17-19]. In contrast, TNF, a pro-inflammatory cytokine released in skin by a variety of cell types including keratinocytes and fibroblasts as well as dermal macrophages and neutrophils, provides a key component of cutaneous anti-viral immune responses. Numerous reports demonstrate, that keratinocyte-derived TNF delivers highly potent signals inducing LC immunogenic function and ability to present antigens [2,18,20-22] and enhances their ability to prime antiviral adaptive immunity [23]. Cross-talk between LC and surrounding keratinocytes, coupled with their ability to cross-present antigens expressed by other cells to skin resident and infiltrating T lymphocytes, defines the major role of LC in skin immunity and allows them to initiate efficient adaptive immune responses in the context of skin infection [5,24,25]. At the same time, continuous trafficking of cutaneous self-antigens by LCs to regional lymph nodes promotes self-tolerance [26,27]. At present, little is known about the genomic mechanisms which programme LC functions in homeostasis and inflammation and how epidermal-derived signals modify such programming.

Like macrophages, LCs originate from yolk-sac progenitors and populate the epidermis during embryonic life. However, functionally, they are more similar to conventional DCs in their ability to efficiently present and cross-present antigens to prime T cell responses [28,29]. Although LCs are among the most efficient antigen presenting cells, their transcriptional networks appear to be distinct from those of both macrophages and DCs [22,30,31], warranting deeper analyses. In all DC subtypes studied, two transcription factors of the interferon regulatory factor (IRF) family, IRF4 and IRF8, have emerged as key players in their development and function [32-36]. IRF4 and IRF8 control a wide range of DC functions. These include induction of innate responses elicited via pattern recognition receptors TLR, NOD, and RIG during viral and bacterial infection [37-39], migration and cell activation, antigen uptake, presentation of MHCI and MHCII-restricted antigens [18,34,40], and the priming of immunogenic as well as tolerogenic CD4 T cell responses [40,41]. Interestingly, the ability of murine DC subsets to efficiently activate CD8 and CD4 T cells, depending on the presentation of antigen in the context of MHC class I and II, is determined by the relative expression of IRF8 and IRF4, respectively[34]. Furthermore, in murine CD8a DCs cross-presentation is critically dependent on BATF3/IRF8 complexes [42-45]. Unlike the case with DCs, murine LC development does not require IRF4 or IRF8 and human LCs can develop in the absence of IRF8 [30,32,46,47]. Nevertheless, the functions of IRF4 and/or IRF8 in regulating the genomic programming of migratory human epidermal LCs remain to be explored.

Here we show using transcriptional and chromatin profiling that migratory LCs are robustly programmed for MHC-I and MHC-II antigen presentation as well as mitochondrial oxidative phosphorylation. LCs express the transcription factors PU.1, IRF4 and BATF3 but not IRF8. LC migration from the epidermis enhances expression of antigen processing components, and the co-stimulatory molecules CD70, CD86 and CD40 and is accompanied by the upregulation of IRF4. TNF stimulation promotes LC cross-presentation while attenuating IRF4 expression. CRISPR-mediated editing reveals IRF4 to positively regulate the LC activation program while repressing NF2EL2 and NFκB pathway genes that promote responsiveness to oxidative stress and inflammatory cytokines. These results suggest that IRF4-dependent genomic programming of human migratory LCs enables their maturation while attenuating excessive inflammatory and immunogenic responses in the epidermis thereby promoting homeostasis. Furthermore, the genomic programming of LCs is independent of IRF8 and instead utilizes IRF4 in combination with PU.1 and BATF3, thereby differentiating LC from conventional dendritic cells.

Results

Analysing human epidermal LCs and their function

To facilitate the analysis of the genomic programming of primary human LCs, we utilized established protocols for isolating highly pure populations of viable and functional LCs from the epidermis [2,22] (Figure 1a-c, Supplementary Figure1). In agreement with our earlier findings and those of others [2,9,10], human LC after migrating from the epidermis underwent maturation and uniformly expressed high levels of CD1a, CD207 and HLA-DR (Figure 1b, Supplementary Figure1a). These LCs express high levels of MHC class II as well as MHC class I complexes on their surface. Furthermore, migration from the epidermis increased LC activation status, as assessed by enhanced expression of co-stimulatory molecules: CD40, CD86 and CD70 (Figure 1c). Such migrated LCs have been shown to efficiently present antigens to CD4 as well as CD8 T cells [2,5,9,10,18,23] (Supplementary Figure1b). However, the effects of migration as well as inflammatory cytokine signalling on the modulation of LC cross-presentation have not been assessed. We therefore use an established model for antigen cross-presentation[2]. Steady state and migrated LCs were pulsed with a 30-amino acid peptide, comprising a 9 amino acid HLA-A2 restricted GLC epitope from Epstein Barr

Virus protein BMLF and stimulated with TNF. We have previously demonstrated that the cross-presentation of the GLC epitope to antigen-specific CD8 T cells was critically dependent on the ability of LCs to take up and actively process the 30AA peptide for presentation [2]. LC migration from the skin induced their ability to cross-present antigens as measured by IFN-γ release from a GLC peptide-specific HLA-A2 CD8 T cell line (Figure 1d, Supplementary Figure1b). TNF signalling further enhanced the ability of migrated LCs to cross-present the same antigen (Figure 1e). We note that in the presence or absence of TNF, cells fixed with glutaraldehyde prior to antigen pulsing did not activate cognate CD8 T cells. In contrast, fixation did not affect presentation of a short peptide, which could be externally loaded onto the MHC molecules. Furthermore, fixing LC post pulsing but before co-culture with T lymphocytes, reduced their ability to activate CD8 T cells[2]. This is consistent with the inhibition of intracellular protein trafficking and antigen processing by glutaraldehyde fixation. Thus, LC migration upregulates CD4 and CD8 T cell co-stimulatory molecules and their antigen presentation as well as cross-presentation capabilities, the latter is augmented by TNF signalling.

Genomic programming of human LCs for antigen presentation

To gain insights into the genomic programming of migrated LCs we analysed their transcriptome using bulk RNA-sequencing. The antigen processing and presentation genes were quantitatively amongst the highest expressed genes in migrated LCs and are therefore designated as the core LC transcriptional programme (Figure 2a). This confirmed and extended our previous analysis using DNA microarrays [22]. We next compared the expression of genes in migrated LCs with previously reported signatures of DCs, including those in the Reactome database and reported by Artyomov and colleagues [29]. These were compiled into antigen processing and antigen cross-presenting molecular signatures (Figure 2b, Supplementary data 1, Supplementary Figure2a). In agreement with previously published data[29], the gene signature encoding antigen processing and presentation in different populations of human skin and blood derived DCs was recapitulated in human LCs, suggesting the existence of a shared transcriptional programme (Figure 2b, Supplementary Figure2a,b). While 53 genes shared between all three subsets encode for proteasome structure (41 genes, FDR $p = 7.32^{-93}$), protein catabolic process, (FDR $p = 8.164^{-100}$) and antigen presentation to class I (FDR $p = 1.324^{-95}$), 287 genes shared between LCs and other

cross-presenting DCs were involved in metabolic processes (FDR p = 5.39^{-19}), including NADH dehydrogenase activity (FDR p = 2.723^{-11}). Notably, the core LC genomic programme was accompanied by high levels of expression of genes encoding ubiquitin protease activity (Figure 2a). Accordingly, 64/66 genes shared between LCs and the antigen processing signature encoded protein ubiquitination components (FDR p = 1.340^{-83}). Importantly, migration from the epidermis also induced high levels of SQSTM1 and TRIM21 proteins, key components involved in antigen processing (Figure 2c).

To uncover genes whose regulated expression could enhance the ability of migrated LCs for antigen cross-presentation, we performed RNA-seq by stimulating with TNF for 2 or 24 hours. As shown before, TNF signalling leads to enhancement of LC antigen cross-presentation (Figure 1e). Although, the overall transcriptional program remained relatively stable under these activation conditions, 1,156 genes were significantly differentially regulated by TNF (EdgeR, FDR<0.05, |LogFC|>1). Transcript-to-transcript clustering (BioLayout Express3D, r= 0.80; MCL = 1.7) identified 7 kinetic clusters with n>8 genes; 3 main clusters were characterised by gene expression peaks at 0, 2 and 24h (Supplementary Figure2 c-e, Supplementary data 2). Gene ontology analysis indicated a consistent shift of the transcriptome towards a more activated LC phenotype; this included reduction of adhesion, enzymatic and trans-membrane signalling with the enhancement of immune functions (Supplementary Figure2c, Supplementary data 2). Two waves of gene activation could be distinguished: an early wave, including the CD40 and CD83 genes, involved in T cell interactions and a late wave including *PSME2* and *TRIM21*, *22* involved in antigen processing and protein ubiquitination (Figure 2d,e, Supplementary data 2). In agreement with our microarray analysis [22], the late wave included components of immunoproteasome (*PSME2*, *ERAP2),* genes involved in intracellular antigen trafficking between the cell membrane, the endosomal compartment and autophagosome (*CAV1*, *SQSTM1*) (Figure 2d,e). Interestingly, this programme also included many members of the superfamily of tripartite motif-containing (TRIM). TRIM proteins are E3 ubiquitin ligases involved in membrane trafficking, protein transport and protein degradation in proteasomes, crucial for many aspects of resistance to pathogens, and reported in the protection against lentiviruses [48,49]. High levels of SQSTM1 and TRIM21 were sustained during stimulation with TNF, together with high levels of expression of co-stimulatory molecules (Supplementary Figure2g,h [2]). Thus, as a consequence of TNF stimulation, the LC transcriptome was highly enriched in genes

involved in antigen processing and MHC I-dependent antigen presentation (Supplementary Figure2c-g)

Coupling of metabolism and antigen presentation in LCs

Next, we used scRNA-seq to analyse the transcriptomes of migrated LCs (>90% of CD1a+, HLADR+ cells). ScanPy analysis of 950 cells clearly identified three major cell clusters (#1-3), confirming LC identity of 916 cells (96.7%) in (ARCHS4 tissues, FDRp = 4.446×10^{-30}, Figure 3a, Supplementary Figure3a-d). The minor clusters 4 and 5 comprise of cells expressing markers of melanocytes and T cells (Supplementary Figure3a,c).

Interestingly, the key genes defining common LC features were *HLADR* and *CD74* that encoding antigen presenting components, together with *TMSB4X,* which is involved in actin polymerisation, cell motility and cytoskeleton re-organisation and *MT-CO2*, *MT-CYB* that encode mitochondrial enzymes (Supplementary Figure3 c,d, Supplementary data 3). Analysis of the pseudotrajectories of cells in clusters 1-3 indicated progression of maturation (Cluster 3 → Cluster 1 → Cluster 2) with an enrichment for expression of genes involved in antigen processing and presentation (*PSMD4*, *PSMD7*, *UBE2L3* cluster 2, Figure 3 b-d, Supplementary Figure3d). Cells in clusters 1 and 2, also displayed expression of a higher proportion of genes involved in oxidative phosphorylation (Figure 3 c-d). The enrichment in genes encoding components of oxidative phosphorylation including cytochrome oxidase function is likely to be highly important for LC biology. The coupling of oxidative phosphorylation with efficient priming of immune responses has been reported previously for murine DCs, increased catabolism was shown to be essential for DC tolerogenic function[50]. Furthermore, mitochondrial membrane potential and ATP production enhances the phagocytic capacity of murine CD8 DCs, augmenting their cross-presentation at a late stage[51]. Thus, migrated LCs appear to be optimally transcriptionally programmed for priming of tolerogenic CD4 and protective CD8 T cell responses.

We next compared the single cell LC transcriptomes with the recently described sub-populations of human blood monocytes and DCs, (GSE94820), [52]), using CellHarmony [53] and SCmap [54] tools. Both mapping strategies confirmed, that the majority of LC single cell transcriptomes were distinct from the conventional DC1, and in contrast resemble cDC2 and cDC3 (Supplementary Figure3e).

Enrichment of IRF composite elements in activate LC promoters

To identify transcription factors involved in the genomic programming of human LCs we perform chromatin profiling and transcription factor motif enrichment analyses. This approach enables the inference of transcriptional regulatory sequences and the transcription factors that are acting to control gene activity in distinct cell types and cell states [40,55]. Notably, tri-methylation of lysine 4 of histone 3 (H3K4Me3) marks active promoters[56], whereas acetylation of lysine 27 of histone 3 (H3K27Ac) marks active transcriptional enhancers; the latter have been postulated to be the primary determinants of tissue-specific gene expression [57,58]. Thus, we performed ChIP-seq to analyse the genome-wide landscape of H3K4Me3 and H3K27Ac in migrated and TNF-activated LCs. Three independent samples of human migrated LCs exhibited a highly conserved histone modification landscape across the genome with overlapping H3K4Me3 peaks in 95% of the marked regions (Supplementary data 4). Analysis of H3K27 acetylation peaks in the same LC preparations shows 78% to be shared across all three samples (Supplementary data 5). Of 13,402 H3K4Me3 peaks that were common to migrated LCs (associated with 11,665 unique genes), over 92% were mapped to promoter regions (Supplementary data 4). In contrast, while 62% of H3K27Ac peaks were positioned either within the promoter region or upstream, a significant proportion of these peaks were distributed within inter- or intragenic regions (Supplementary data 5). This distribution was expected for intergenic or intronic enhancers that function at large distances from the promoters on which they act.

Focusing the analysis on genes associated with immune function (InnateDB: Immunome collection [59], we identified 290 immune genes with active (H3K4Me3) promoters. These were highly enriched in genes encoding receptor binding and activation (in particular able to respond to TNF cytokine family signalling (FDR p= $1.2x10^{-12}$), and genes involved in antigen processing and presentation (FDR p = 10^{-22}). As noted above, considerable overlap between H3K4Me3 and H3K27Ac marks was apparent at promoter regions. This indicated that migrated LCs are pre-programmed for efficient antigen processing and presentation (Supplementary Figure4 a-c). In concordance with the observed gene expression pattern, histone marks were very low or absent on genes involved in innate inflammatory responses, such as production of cytokines (Supplementary data, 4,5). To analyse whether genomic programming of human migrated LCs was similar to other known cell types including monocytes, DCs and macrophages, we compared our ChiP-seq profiles

to a large collection of publically available genomics datasets (see Methods). Surprisingly, the chromatin landscape of migrated LCs was strikingly similar to that of macrophages and CD14+ monocytes, and significantly less strongly correlated with that of dendritic cells (Supplementary data Table6).

Stimulation with TNF preserved H3K27Ac acetylation in genes underpinning LC activation (Figure 4 a,b). Two hours after TNF exposure, the high levels of H3K27 acetylation, observed in steady state LCs (Figure 4a) were maintained for 90% and 92% of genes induced during the early (cluster 3) and late (cluster 2) waves of responses, respectively (Figure 4a). Moreover, TNF signalling enhanced H3K27Ac levels in over 50% of genes (SupplementaryFigure4a). In line with the transcriptome changes, genes with enhanced H3K27Ac marks at 2h encoded innate immune processes including leukocyte activation (FDR p-value = $2x10^{-19}$) and co-stimulation (FDR p-value = $7.99x10^{-16}$). A significant proportion of genes (286) within this programme was associated with ubiquitin-mediated proteolysis, highlighting the importance of this process for LC function (FDR p = 3.8×10^{-85}). In contrast, genes involved in cell cycle and motility were characterised by reduced histone acetylation marks. It is worth noting that the majority of histone marks induced by TNF signalling were readily detected prior to activation (Figure 4a,b, Supplementary Figure4a-c), suggesting that the migrated LCs were pre-programmed for rapid immune activation from a genomic standpoint.

To infer transcription factors directly controlling the transcriptional programmes in human LCs, we performed TF motif enrichment analyses, revealing an extremely high enrichment of the composite Interferon Regulatory Factor-binding (IRF-binding) sequences [36] at the promoters of genes carrying H3K4Me3 and H3K27Ac marks (Figure 4c). The ETS-Interferon Composite Element (EICE) was the most frequent and significantly enriched TF motif in steady state migrated LCs (47%, -logp=16,020), while the AP1-Interferon Composite Element (AICE) and the interferon-stimulated response element (ISRE/IRF1) were present at frequencies of 13.6% (-logp=4788) and 10.3% (-logp=3.156), respectively (Figure 4c, Supplementary data 7). Analysis of biological processes enriched for genes carrying H3K4Me3 and H3K27Ac marks in their promoter regions and predicted IRF4,8 binding motifs demonstrated, that over 60% were involved in protein polyubiquitination, or antigen processing and presentation (Figure 4d, Supplementary Figure4d). Thus, transcription and chromatin profiling coupled with TF motif analysis strongly suggested that IRF4 or IRF8 in

conjunction with PU.1 and BATF3, binding to EICE and AICE motifs, respectively, could program the expression of a large set of genes in human LCs.

LC migration and maturation associate with IRF4 not IRF8

Given critical roles for specific members of the IRF, ETS and AP-1 family transcription factors in antigen presentation in conventional DCs[42,60], and the enrichment of EICE and AICE composite motifs in active chromatin regions of LCs, we analysed the expression of IRF4, IRF8, PU.1, SPIB, cJUN, JUND and BATF3, in steady-state and migrated LCs. Whereas IRF4 and BATF3 proteins were expressed in steady-state LCs surprisingly there was no detectable expression of IRF8 (Figure 5a, Supplementary Figure5 a-f). Importantly, migration out of the skin further induced IRF4 expression (Figure 5a,b). In contrast, IRF8 protein remained undetectable in migrated LCs (Figure 5a). Analysis of transcripts for these transcription factors was in keeping with the expression of their proteins (Figure 5c, Supplementary Figure5a-f). We note that transcripts encoding *IRF4*, *PU.1* (Spi1) and *cJUN* were most highly expressed in LCs and were at least an order of magnitude greater than those encoding *IRF8* and the PU.1 paralog *SpiB*. TNF stimulation maintained the expression of BATF3 protein while downregulating IRF4. Notably, IRF8 protein remained undetectable over the time course of TNF stimulation, in spite of low level up-regulation of IRF8 mRNA (Figure 5c, 5d, Supplementary Figure5f). Thus, the genomic programming of human LCs and also their ability to cross-present antigens appears to be IRF8 independent. Instead, the results strongly suggest that human LCs depend on IRF4 along with PU.1 and BATF3 for transcriptional programmes underpinning their contextual functions including expression of antigen cross-presentation genes.

IRF4 balances LC maturation and inflammatory signalling

Given that IRF4 is upregulated when LCs migrate from the epidermis (Figure 5 a,b), a process associated with their maturation as well as enhanced antigen cross-presentation (Figure 1d), we wished to determine how perturbation of IRF4 impacts the genomic programming of migrated LCs. CRISPR-Cas9 editing with an IRF4 guide-Cas9 complex was used to knock down IRF4 expression in migrated LCs (Figure 6a,b, Supplementary Figure 6a). Importantly, transfection of LCs by nucleofection did not lead to enhanced cell death (Supplementary Figure 6b). The effect of genome editing was sustained at 72h and 96h post

nucleofaction, however the cell viability decreased with time both in the knock-down and in the control cells. scRNA-seq of 1000 control (wild-type, WT) and 1000 edited (knock-down, KD) cells confirmed significantly lower levels of IRF4 expression at the mRNA level, and separation of transcriptomes of KD and control cells in the uMAP plot (Figure 6c, Supplementary Figure6c).

Comparison of transcriptomes of WT and KD LCs demonstrated importance of IRF4 for regulation of key processes in LCs. IRF4 KD LCs were impaired for expression of genes involved in myeloid leukocyte activation, including *LYZ:* antimicrobial function, *CTSH*: antigen processing and *WFDC21P*: a long non-coding RNA implicated in DC differentiation, FDR p = 1.25^{-4}) as well as cellular metal ion homeostasis (FDR p=1.22^{-4}). Interestingly, expression of genes encoding ubiquitin pathway components (ubiquitin protein ligase binding, FDR p=2.80^{-2}) was also diminshed. These genes showed strong overlap with genes carrying H3K4Me3 and H3K27Ac marks (Supplementary data 4,5,8). Strikingly, IRF KD LCs manifested increased expression of genes encoding responsiveness to cytokines (FDR p = 1.52^{-13}) and cellular stress, including oxidative stress (FDR p= 8.98^{-12}), with induction of *NFkB1, MAP4K4, NFL2F1 and NFL2F2* (Figure 6d-f, Supplementary Figure6c,d, Supplementary data 8, 9). Thus IRF4 positively regulates genes involved in LC maturation while attenuating those involved in inflammatory cytokine and oxidative stress signalling.

Discussion

Since their discovery by Paul Langerhans in 1864, LCs have been puzzling scientists. Despite being the longest studied antigen presenting cell population, and being considered the stereotypical dendritic cells, their place in the innate immune cell spectrum has remained elusive. This is due to the difficulties in studying LC, arising from paucity of *in vitro* models, controversy around defining a LC progenitor, and the differences between human and murine skin immunology [61]. To address these challenges we analysed primary human LCs, using bulk and single-cell RNAseq as well as H3K4Me3 and H4K27Ac ChIPseq and couple these genomic and epigenomic profiles with LC phenotypic and functional characteristics. Our extensive transcriptomic and epigenomic analyses of primary human skin-derived LCs reveals three striking features: (i) the pre-programming of LC chromatin and transcriptome landscapes (ii) the importance of migration from the epidermis for activation of the LC maturation and (iii) the key role of a major immune transcriptional regulator IRF4 rather

than its paralog IRF8. We suggest all three features are likely to be inter-connected, and dictated by the localisation of LCs in the epidermis and their functions in maintaining immune homeostasis [62].

By profiling the H3K4Me3 and H3K27Ac histone modifications across the LC genome, we were able to analyse the chromatin landscape of human migrated LCs for the first time, and document that their genomic programme encompassing antigen presentation genes is poised for efficient expression during, or before their migration from the epidermis. TNF, a pro-inflammatory cytokine produced in the skin plays a critical role in inducing LC immunogenic function and ability to present antigens. Stimulation with TNF, significantly enhanced the pre-existing transcriptional programme, further confirming that the LCs are fully committed for efficient antigen presentation as well as cross-presentation. Such genomic programming, realised at the level of transcriptional enhancers, could be both developmentally and environmentally specified. [63]

We have delineated three distinctive IRF-binding motifs, EICE, AICE and ISRE as key regulatory elements associated with expression of the LC transcriptional programme. Classically, EICE and AICE have been shown to be bound by IRF4 or IRF8, in combination with their transcriptional partners from either ETS or AP-1 transcription factor families [36,64-67]. Our analysis of IRF4 and IRF8 protein expression and their transcriptional binding partners clearly demonstrates that IRF8 protein is not detectably expressed in human LCs and is thus dispensable for their function, including cross-presentation of exogenous antigens to CD8 T cells. IRF8 has been implicated as a key transcription factor in murine CD8alpha+ DCs regulating genes involved in cross-presentation through interaction with BATF on composite elements (AICE) in the promoters of target genes [42,45]. By contrast, recent reports in other cell types, such as MoDCs[68] and cDC2 (K. Murphy, personal communication) indicate that the same transcriptional programme can be regulated by IRF4[68]. Hence the high levels of IRF4 expressed in human migrated LCs, are likely to be involved in the orchestration of this programme[68].

The analysis of LCs edited for expression of IRF4 using a CRISP-Cas9 system allowed us to directly test the importance of IRF4 in the transcriptional programming of human LCs. In concordance with studies by Chopin and colleagues [30,47], IRF4 was not critical for LC survival. However, we demonstrated that LC genomic programming was critically dependent on IRF4 function. Knockdown of IRF4 resulted in the impaired expression of genes involved

in LC activation, homeostasis as well as ubiquitin dependent antigen processing pathways. Strikingly, knockdown of IRF4 resulted in the increased expression of genes encoding multiple components of the NFκB and NF2EL2 pathways that control responsive to inflammatory cytokines such as TNF and oxidative stress. Thus, IRF4 appears to dampen the response of LCs to inflammatory cytokines and in so doing may promote tolerogenic responses in the skin. Such a function for IRF4 in dendritic cells in priming Treg responses has been previously observed in murine system [40]. The balance between efficient antigen presentation and responsiveness to inflammatory signalling appears to be critical for LC biology. One of the key functions of LCs is maintenance of peripheral tolerance in situ [5] and through continuous trafficking of cutaneous self-antigens to regional lymph nodes [26,27]. In contrast, upon exposure to pro-inflammatory cytokines, cross-presentation of antigens by LCs plays important role for adaptive immune responses [10,22,24]. We note that, in parallel with enhancing LC ability to stimulate CD8 T cells, TNF signalling in LCs down regulated the expression of IRF4 protein. Thus, we propose that a reciprocal feedback inhibition loop between inflammatory cytokines and IRF4 may be critical for balancing tolerogenic versus immunogenic LC responses in the epidermis.

[2,22,69-72]The notable lack of IRF8 expression in LCs, consistent with inactive chromatin at the IRF8 locus, distinguishes LCs from both macrophages and DCs and likely contributes to their discrete role in epidermal homeostasis. Independence of LCs from IRF8 could represent a mechanism for their plasticity, enabling them to be adapted to their environmental niche. IRF8 has been shown to regulate production of pro-inflammatory cytokines in DCs [73,74], and macrophages, the latter contributing to chronic inflammation[75]. We propose that by utilising IRF4 rather than IRF8, LCs uncouple the cross-presentation of antigens from production of pro-inflammatory mediators, and thus prevent excessive inflammatory responses and promote epidermal homeostasis. It is plausible that the increase in IRF4 expression during LC migration out of the epidermis makes LCs immunocompetent, in a highly controlled manner, activating IRF4-coordinated transcriptomic programmes centred around efficient antigen presentation but independent of NFkB1/MAPK4K signalling. These observations along with our earlier analysis of IRF4 function in murine DCs[40] lead us to propose a context-dependent model of LC activation, where loss of contact with epidermal structural cells upregulates IRF4 expression and initiates an LC activation programme that promotes tolerogenic T cell responses and

436 immune homeostasis. Signalling by pro-inflammatory cytokines attenuates IRF4 expression
437 and elicits a transcriptomic programme that more effectively primes immunogenic T cell
438 responses.
439
440

Methods

Cell isolation and stimulation with TNF

Skin specimens and blood samples were acquired from healthy individuals after obtaining informed written consent with approval by the Southampton and South West Hampshire Research Ethics Committee in adherence to Helsinki Guidelines [ethical approvals: 07/Q1704/59, NRES 07 Q1704 46]. Split skin was obtained using graft knife and subjected to dispase (2U/ml, Gibco, UK, 20h, +4℃) digestion of epidermal sheets. Migrated LCs were harvested after 48 hours culture of epidermal fragments in full culture media (RPMI, Gibco, UK, 5%FBS, Invitrogen, UK, 100 IU/ml penicillin and 100 mg/ml streptomycin, Sigma, UK). Low density cells were enriched using density gradient centrifugation (Optiprep 1:4.2, Axis Shield, Norway[2] and purified with CD1a+ magnetic beads according to manufacturer's protocol (Milenyi Biotec, UK). Migrated LCs were processed for RNA-seq and ChIP-seq experiment or immediately cryopreserved in 90% FBS (Gibco, UK), 10% DMSO (Sigma, UK). For genomic and transcriptomic analyses of activated LCs fresh migrated LCs from 3 donors were stimulated with TNF (25 ng/ml, Miltenyi Biotec, UK) for 2, and 24 hours (RNA-seq: 3 x 10^5 cells/donor/time point, ChIP-seq: 1.5-2 x 10^6 cells/donor/time point, paired samples from the same donor for RNA-seq and ChIP-seq). Steady-state LCs were enzymatically digested from the epidermal sheets using Liberase™ TM research grade (Roche, UK, 2h at 37℃).

Antigen cross-presentation assay

Cells were pulsed with 10 μM proGLC (FNNFTVSFWLRVPKVSASHLEGLCTLVAML; Peptide Protein Research, Fareham, UK) for 24 hours, supplemented with TNF (25 ng/ml, Miltenyi Biotec, UK) after initial 2 hours. Human responder cells: PBMC from HLA-A2 individuals were isolated by Ficoll-Hypaque density gradient centrifugation and co-cultured with 40 µM EBV peptide for 12 days in complete medium supplemented with 1% sodium pyruvate (Gibco, UK) plus 10% human serum (Sigma,UK). IL-2 (100 IU/ml, Peprotech, UK) was added every 3 days. This method expands the pool of GLC-specific CD8 T cells to 30% (assessed by tetramer assay and ELISpot assay Polak et al 2012[2]). IL-2 was removed from the culture for 24 hours prior to testing in ELISpot. For ELISpot assays, TNF matured and washed EBV peptide pulsed LCs ($1x10^3$ cells) were co-cultured with GLC peptide-specific T cells ($5x10^4$

cells/ per well) for 20 hours as per manufacturer's protocol (Mabtech, Sweden).

Flow cytometry

All antibodies were used at pre-titrated, optimal concentrations. For surface staining of live cells buffer containing 5% FBS and 1% BSA was used for all antibody staining. FACS Aria flow cytometer (Becton Dickinson, USA) was used for analysis of human LCs for the expression of CD207, CD1a, HLA-DR (mouse monoclonal antibodies, CD1a, CD207:Miltenyi Biotech, UK and HLA-DR: BD Biosciences, UK). For transcription factor intra-nuclear staining cells were permeabilised with Foxp3 / Transcription Factor Staining Buffer Set (eBiosciences, UK) accordingly to the manufacturer protocol, and stained with monoclonal antibodies targeting IRF4, IRF8, BATF3, PU.1, cJUN, (IRF4:rat monoclonal, eBiosciences, UK, mouse monoclonal: IRF8, eBiosciences, BATF, R&D Systems, JUN Millimark, UK, PU.1 Biolegend, UK). IRF1 staining was done using rabbit polyclonal anti-human IRF1 antibody (Abcam, UK) following fixation with 80% methyl-alcohol and permeabilisation with Tween20. Analysis was performed on live AQUA-negative (Invitrogen, UK), CD207+/HLADR+ migrated or steady-state LCs, in comparison with appropriate isotype controls.

RNA-seq

RNA was isolated using RNeasy mini kit (Qiagen) as per the manufacturer's protocol. RNA concentration and integrity was determined with an Agilent Bioanalyser (Agilent Technologies, Santa Clara, CA). All the samples had a RNA integrity number of 7.0 or above and were taken forward for labelling. RNA-seq libraries were generated from 300 ng total RNA with an RNA Sample Prep Kit (Illumina) according to a standard protocol. The libraries were sequenced with Illumina HiSeq2500 in the DNA sequencing core of the Cincinnati Children's Hospital Medical Center. Each sample was used to generate 2×10^7 reads with 75–base pair paired-end sequencing.

RT-qPCR

The expression of chosen genes was validated with quantitative PCR, using the TaqMan gene expression assays for target genes: YWHAZ (HS03044281_g1), CAV1 (Hs00971716_m1), PSME2 (Hs01923165_u1), (Applied Biosystems, Life Technologies, Paisley, UK) in cells from independent donors. RNA extraction (RNeasy micro kit, Qiagen)

503 and reverse transcription (High-Capacity cDNA Reverse Transcription Kit with RNAse
504 inhibitors, Applied Biosystems, Life Technologies, Paisley, UK) were carried out accordingly
505 to the manufacturer's protocol.
506
507 **ChIP-seq**
508
509 Purified migrated LCs were fixed with 1% formaldehyde for 15 min and the reaction
510 quenched with 0.125 M glycine. Chromatin was isolated by the addition of lysis buffer,
511 followed by disruption with a Dounce homogenizer. Lysates were sonicated and the DNA
512 sheared to an average length of 100–200 bp (Covaris). Genomic DNA (Input) was prepared
513 by treating aliquots of chromatin with RNase, proteinase K and heat to remove crosslinks,
514 followed by ethanol precipitation. Pellets were resuspended and the resulting DNA was
515 quantified on a NanoDrop spectrophotometer. Extrapolation to the original chromatin
516 volume allowed quantitation of the total chromatin yield. Genomic DNA regions of interest
517 were isolated using 2.8 µg of antibody against H3K27Ac or H3K4Me3[76]. Complexes were
518 washed, eluted from the beads with SDS buffer, and subjected to RNase and proteinase K
519 treatment. Crosslinks were reversed by incubation overnight at 65 °C, and ChIP DNA was
520 purified by phenol–chloroform extraction and ethanol precipitation. Illumina sequencing
521 libraries were prepared from the ChIP and input DNAs by the standard consecutive
522 enzymatic steps of end- polishing, dA-addition, and adaptor ligation using Truplex^{TM} –FD
523 prep kit (Rubicon Genomics, USA). After a final PCR amplification step, the resulting DNA
524 libraries were quantified using Qubid and 75 nucleotide single-end reads were sequenced
525 Illumina HiSeq2500 in the DNA sequencing core of the Cincinnati Children's Hospital Medical
526 Center.

527 **Drop-seq**
528
529 Highly purified human LCs (> 80% of CD1a+HLADR+) were unbanked from cryo-storage, and
530 processed on ice to enable the co-encapsulation of single cells with genetically-encoded
531 beads (Drop-seq, [77]). Monodisperse droplets at 1 nl in size were generated using the
532 microfluidic devices fabricated in the Centre for Hybrid Biodevices, University of
533 Southampton. To achieve single cell/single bead encapsulation barcoded Bead SeqB
534 [Chemgenes, USA], microfluidics parameters (pump flow speeds for cells and bead inlets,

cell buoyancy) were adjusted to optimise cell-bead encapsulation and the generation of high quality cDNA libraries. Following encapsulation, ~4500 STAMPS (beads exposed to a single cell) from 1.2 ml cell suspension were generated in the Faculty of Medicine University of Southampton Drop-seq Facility. Based on encapsulation frequencies and bead counts up to 1000 STAMPS were taken further for library prep (High Sensitivity DNA Assay, Agilent Bioanalyser, 12 peaks with the average fragment size 500 bp). The resulting libraries were run on a shared NextSeq run ($1.5x10^5$ reads for maximal coverage) at the Wessex Investigational Sciences Hub laboratory, University of Southampton, to obtain single cell sequencing data.

Bioinformatic analysis of sequencing data

All sequencing data have been analysed using established bioinformatic pipelines. For full description please see the Supplementary Methods.

CRISPR-Cas9 gene editing

Primary human migrated LCs were subjected to nucleofection (185,000 cells/20µl P3 reagent per reaction, Lonza protocol EH104) with purified *S. pyogenes* Cas9 (spCas9) complexed with a modified single guide RNAs (sgRNAs) targeting *IRF4* (Synthego, C*G*C*AGGCGCGUCUUCCAG*G*U*). sgRNAs had the following modifications to increase stability: 2'-O-methyl analogs and 3' phosphorothioate internucleotide linkages at the first three 5' and 3' terminal RNA residues. Ribonucleoprotein complexes were prepared in 1:6 (vol:vol) ratio (protein to modified RNA oligonucleotide) in ddH_2O immediately prior to nucleofection. Following culture (24-96h) cell viability and IRF4 expression at the protein level was assessed by flow cytometry. scRNA-sequencing using DropSeq encapsulation was carried out on 1000 control and 1000 edited primary LCs cells at 48h time point.

Data Availability: Sequencing data for RNA-seq, scRNA-seq and ChiP-seq is stored in Gene Expression Omnibus database, submission number GSE120386:

https://www.ncbi.nlm.nih.gov/geo/query/acc.cgi?acc=GSE120386

References

1 van der Vlist, M. *et al.* Human Langerhans cells capture measles virus through Langerin and present viral antigens to CD4(+) T cells but are incapable of cross-

presentation. *European journal of immunology* **41**, 2619-2631, doi:10.1002/eji.201041305 (2011).

2 Polak, M. E. *et al.* CD70-CD27 interaction augments CD8+ T-cell activation by human epidermal Langerhans cells. *The Journal of investigative dermatology* **132**, 1636-1644, doi:10.1038/jid.2012.26 (2012).

3 Ribeiro, C. M. *et al.* Receptor usage dictates HIV-1 restriction by human TRIM5alpha in dendritic cell subsets. *Nature* **540**, 448-452, doi:10.1038/nature20567 (2016).

4 van Dalen, R. *et al.* Langerhans Cells Sense Staphylococcus aureus Wall Teichoic Acid through Langerin To Induce Inflammatory Responses. *mBio* **10**, doi:10.1128/mBio.00330-19 (2019).

5 Seneschal, J., Clark, R. A., Gehad, A., Baecher-Allan, C. M. & Kupper, T. S. Human epidermal Langerhans cells maintain immune homeostasis in skin by activating skin resident regulatory T cells. *Immunity* **36**, 873-884, doi:10.1016/j.immuni.2012.03.018 (2012).

6 Toews, G. B., Bergstresser, P. R. & Streilein, J. W. Epidermal Langerhans cell density determines whether contact hypersensitivity or unresponsiveness follows skin painting with DNFB. *Journal of immunology* **124**, 445-453 (1980).

7 Kubo, A., Nagao, K., Yokouchi, M., Sasaki, H. & Amagai, M. External antigen uptake by Langerhans cells with reorganization of epidermal tight junction barriers. *The Journal of experimental medicine* **206**, 2937-2946, doi:10.1084/jem.20091527 (2009).

8 Berle, E. J., Braathen, L. R. & Thorsby, E. HLA-D/DR restriction of Langerhans cell-dependent antigen activation of T lymphocytes. The same D/DR determinants are restriction elements on monocytes and Langerhans cells. *Scandinavian journal of immunology* **16**, 549-552, doi:10.1111/j.1365-3083.1982.tb00758.x (1982).

9 Banchereau, J. *et al.* The differential production of cytokines by human Langerhans cells and dermal CD14(+) DCs controls CTL priming. *Blood* **119**, 5742-5749, doi:10.1182/blood-2011-08-371245 (2012).

10 Klechevsky, E. *et al.* Functional specializations of human epidermal Langerhans cells and CD14+ dermal dendritic cells. *Immunity* **29**, 497-510, doi:10.1016/j.immuni.2008.07.013 (2008).

11 Sigal, L. J., Crotty, S., Andino, R. & Rock, K. L. Cytotoxic T-cell immunity to virus-infected non-haematopoietic cells requires presentation of exogenous antigen. *Nature* **398**, 77-80, doi:10.1038/18038 (1999).

12 Huang, A. Y. *et al.* Role of bone marrow-derived cells in presenting MHC class I-restricted tumor antigens. *Science (New York, N.Y.)* **264**, 961-965, doi:10.1126/science.7513904 (1994).

13 Liu, L. *et al.* Vaccinia virus induces strong immunoregulatory cytokine production in healthy human epidermal keratinocytes: a novel strategy for immune evasion. *Journal of virology* **79**, 7363-7370, doi:10.1128/jvi.79.12.7363-7370.2005 (2005).

14 Borkowski, T. A. *et al.* A role for TGFbeta1 in langerhans cell biology. Further characterization of the epidermal Langerhans cell defect in TGFbeta1 null mice. *The Journal of clinical investigation* **100**, 575-581, doi:10.1172/jci119567 (1997).

15 Kel, J. M., Girard-Madoux, M. J., Reizis, B. & Clausen, B. E. TGF-beta is required to maintain the pool of immature Langerhans cells in the epidermis. *Journal of immunology* **185**, 3248-3255, doi:10.4049/jimmunol.1000981 (2010).

16 Yasmin, N. *et al.* beta-Catenin Promotes the Differentiation of Epidermal Langerhans Dendritic Cells. *The Journal of investigative dermatology* **133**, 1250-1259, doi:10.1038/jid.2012.481 (2013).
17 Ebner, S. *et al.* Thymic stromal lymphopoietin converts human epidermal Langerhans cells into antigen-presenting cells that induce proallergic T cells. *The Journal of allergy and clinical immunology* **119**, 982-990, doi:10.1016/j.jaci.2007.01.003 (2007).
18 Polak, M. E., Ung, C. Y., Masapust, J., Freeman, T. C. & Ardern-Jones, M. R. Petri Net computational modelling of Langerhans cell Interferon Regulatory Factor Network predicts their role in T cell activation. *Scientific reports* **7**, 668, doi:10.1038/s41598-017-00651-5 (2017).
19 Soumelis, V. *et al.* Human epithelial cells trigger dendritic cell mediated allergic inflammation by producing TSLP. *Nature immunology* **3**, 673-680, doi:10.1038/ni805 (2002).
20 Cumberbatch, M., Bhushan, M., Dearman, R. J., Kimber, I. & Griffiths, C. E. IL-1beta-induced Langerhans' cell migration and TNF-alpha production in human skin: regulation by lactoferrin. *Clinical and experimental immunology* **132**, 352-359 (2003).
21 Berthier-Vergnes, O. *et al.* TNF-alpha enhances phenotypic and functional maturation of human epidermal Langerhans cells and induces IL-12 p40 and IP-10/CXCL-10 production. *FEBS letters* **579**, 3660-3668, doi:10.1016/j.febslet.2005.04.087 (2005).
22 Polak, M. E. *et al.* Distinct molecular signature of human skin langerhans cells denotes critical differences in cutaneous dendritic cell immune regulation. *The Journal of investigative dermatology* **134**, 695-703, doi:10.1038/jid.2013.375 (2014).
23 Epaulard, O. *et al.* Macrophage- and Neutrophil-Derived TNF-alpha Instructs Skin Langerhans Cells To Prime Antiviral Immune Responses. *Journal of immunology* **193**, 2416-2426, doi:10.4049/jimmunol.1303339 (2014).
24 Stoitzner, P. *et al.* Langerhans cells cross-present antigen derived from skin. *Proceedings of the National Academy of Sciences of the United States of America* **103**, 7783-7788, doi:10.1073/pnas.0509307103 (2006).
25 Jiang, X. *et al.* Skin infection generates non-migratory memory CD8+ T(RM) cells providing global skin immunity. *Nature* **483**, 227-231, doi:10.1038/nature10851 (2012).
26 Kitashima, D. Y. *et al.* Langerhans Cells Prevent Autoimmunity via Expansion of Keratinocyte Antigen-Specific Regulatory T Cells. *EBioMedicine* **27**, 293-303, doi:10.1016/j.ebiom.2017.12.022 (2018).
27 Hemmi, H. *et al.* Skin antigens in the steady state are trafficked to regional lymph nodes by transforming growth factor-beta1-dependent cells. *International immunology* **13**, 695-704, doi:10.1093/intimm/13.5.695 (2001).
28 Doebel, T., Voisin, B. & Nagao, K. Langerhans Cells - The Macrophage in Dendritic Cell Clothing. *Trends in immunology* **38**, 817-828, doi:10.1016/j.it.2017.06.008 (2017).
29 Artyomov, M. N. *et al.* Modular expression analysis reveals functional conservation between human Langerhans cells and mouse cross-priming dendritic cells. *The Journal of experimental medicine* **212**, 743-757, doi:10.1084/jem.20131675 (2015).
30 Chopin, M. & Nutt, S. L. Establishing and maintaining the Langerhans cell network. *Seminars in cell & developmental biology* **41**, 23-29, doi:10.1016/j.semcdb.2014.02.001 (2015).

31 Clayton, K., Vallejo, A. F., Davies, J., Sirvent, S. & Polak, M. E. Langerhans Cells-Programmed by the Epidermis. *Frontiers in immunology* **8**, 1676, doi:10.3389/fimmu.2017.01676 (2017).
32 Tamura, T. *et al.* IFN regulatory factor-4 and -8 govern dendritic cell subset development and their functional diversity. *Journal of immunology* **174**, 2573-2581 (2005).
33 Gabriele, L. & Ozato, K. The role of the interferon regulatory factor (IRF) family in dendritic cell development and function. *Cytokine & growth factor reviews* **18**, 503-510, doi:10.1016/j.cytogfr.2007.06.008 (2007).
34 Vander Lugt, B. *et al.* Transcriptional programming of dendritic cells for enhanced MHC class II antigen presentation. *Nature immunology*, doi:10.1038/ni.2795 (2013).
35 Tussiwand, R. *et al.* Compensatory dendritic cell development mediated by BATF-IRF interactions. *Nature* **490**, 502-507, doi:10.1038/nature11531 (2012).
36 Glasmacher, E. *et al.* A genomic regulatory element that directs assembly and function of immune-specific AP-1-IRF complexes. *Science (New York, N.Y.)* **338**, 975-980, doi:10.1126/science.1228309 (2012).
37 Honda, K. & Taniguchi, T. IRFs: master regulators of signalling by Toll-like receptors and cytosolic pattern-recognition receptors. *Nature reviews. Immunology* **6**, 644-658, doi:10.1038/nri1900 (2006).
38 Fortier, A., Doiron, K., Saleh, M., Grinstein, S. & Gros, P. Restriction of Legionella pneumophila replication in macrophages requires concerted action of the transcriptional regulators Irf1 and Irf8 and nod-like receptors Naip5 and Nlrc4. *Infection and immunity* **77**, 4794-4805, doi:10.1128/iai.01546-08 (2009).
39 Zhao, T. *et al.* The NEMO adaptor bridges the nuclear factor-kappaB and interferon regulatory factor signaling pathways. *Nature immunology* **8**, 592-600, doi:10.1038/ni1465 (2007).
40 Vander Lugt, B. *et al.* Transcriptional determinants of tolerogenic and immunogenic states during dendritic cell maturation. *The Journal of cell biology* **216**, 779-792, doi:10.1083/jcb.201512012 (2017).
41 Bajana, S., Roach, K., Turner, S., Paul, J. & Kovats, S. IRF4 promotes cutaneous dendritic cell migration to lymph nodes during homeostasis and inflammation. *Journal of immunology* **189**, 3368-3377, doi:10.4049/jimmunol.1102613 (2012).
42 Hildner, K. *et al.* Batf3 deficiency reveals a critical role for CD8alpha+ dendritic cells in cytotoxic T cell immunity. *Science (New York, N.Y.)* **322**, 1097-1100, doi:10.1126/science.1164206 (2008).
43 Segura, E. & Amigorena, S. Cross-Presentation in Mouse and Human Dendritic Cells. *Advances in immunology* **127**, 1-31, doi:10.1016/bs.ai.2015.03.002 (2015).
44 Aliberti, J. *et al.* Essential role for ICSBP in the in vivo development of murine CD8alpha + dendritic cells. *Blood* **101**, 305-310, doi:10.1182/blood-2002-04-1088 (2003).
45 Sichien, D. *et al.* IRF8 Transcription Factor Controls Survival and Function of Terminally Differentiated Conventional and Plasmacytoid Dendritic Cells, Respectively. *Immunity* **45**, 626-640, doi:10.1016/j.immuni.2016.08.013 (2016).
46 Hambleton, S. *et al.* IRF8 mutations and human dendritic-cell immunodeficiency. *The New England journal of medicine* **365**, 127-138, doi:10.1056/NEJMoa1100066 (2011).

47 Chopin, M. *et al.* Langerhans cells are generated by two distinct PU.1-dependent transcriptional networks. *The Journal of experimental medicine* **210**, 2967-2980, doi:10.1084/jem.20130930 (2013).

48 Ozato, K., Shin, D. M., Chang, T. H. & Morse, H. C., 3rd. TRIM family proteins and their emerging roles in innate immunity. *Nature reviews. Immunology* **8**, 849-860, doi:10.1038/nri2413 (2008).

49 Hatakeyama, S. TRIM Family Proteins: Roles in Autophagy, Immunity, and Carcinogenesis. *Trends in biochemical sciences* **42**, 297-311, doi:10.1016/j.tibs.2017.01.002 (2017).

50 Everts, B. & Pearce, E. J. Metabolic control of dendritic cell activation and function: recent advances and clinical implications. *Frontiers in immunology* **5**, 203, doi:10.3389/fimmu.2014.00203 (2014).

51 Chougnet, C. A. *et al.* Loss of Phagocytic and Antigen Cross-Presenting Capacity in Aging Dendritic Cells Is Associated with Mitochondrial Dysfunction. *Journal of immunology* **195**, 2624-2632, doi:10.4049/jimmunol.1501006 (2015).

52 Villani, A. C. *et al.* Single-cell RNA-seq reveals new types of human blood dendritic cells, monocytes, and progenitors. *Science (New York, N.Y.)* **356**, doi:10.1126/science.aah4573 (2017).

53 DePasquale, E. A. K. *et al.* cellHarmony: cell-level matching and holistic comparison of single-cell transcriptomes. *Nucleic acids research* **47**, e138, doi:10.1093/nar/gkz789 (2019).

54 Kiselev, V. Y., Yiu, A. & Hemberg, M. scmap: projection of single-cell RNA-seq data across data sets. *Nature methods* **15**, 359-362, doi:10.1038/nmeth.4644 (2018).

55 Barski, A. *et al.* High-resolution profiling of histone methylations in the human genome. *Cell* **129**, 823-837, doi:10.1016/j.cell.2007.05.009 (2007).

56 Heintzman, N. D. *et al.* Histone modifications at human enhancers reflect global cell-type-specific gene expression. *Nature* **459**, 108-112, doi:10.1038/nature07829 (2009).

57 Buecker, C. & Wysocka, J. Enhancers as information integration hubs in development: lessons from genomics. *Trends in genetics : TIG* **28**, 276-284, doi:10.1016/j.tig.2012.02.008 (2012).

58 Creyghton, M. P. *et al.* Histone H3K27ac separates active from poised enhancers and predicts developmental state. *Proceedings of the National Academy of Sciences of the United States of America* **107**, 21931-21936, doi:10.1073/pnas.1016071107 (2010).

59 Breuer, K. *et al.* InnateDB: systems biology of innate immunity and beyond--recent updates and continuing curation. *Nucleic acids research* **41**, D1228-1233, doi:10.1093/nar/gks1147 (2013).

60 Vander Lugt, B. *et al.* Transcriptional programming of dendritic cells for enhanced MHC class II antigen presentation. *Nature immunology* **15**, 161-167, doi:10.1038/ni.2795 (2014).

61 Mestas, J. & Hughes, C. C. Of mice and not men: differences between mouse and human immunology. *Journal of immunology* **172**, 2731-2738, doi:10.4049/jimmunol.172.5.2731 (2004).

62 Schuster, C. *et al.* Phenotypic characterization of leukocytes in prenatal human dermis. *The Journal of investigative dermatology* **132**, 2581-2592, doi:10.1038/jid.2012.187 (2012).

63 Kaufmann, E. *et al.* BCG Educates Hematopoietic Stem Cells to Generate Protective Innate Immunity against Tuberculosis. *Cell* **172**, 176-190.e119, doi:10.1016/j.cell.2017.12.031 (2018).
64 Li, P. *et al.* BATF-JUN is critical for IRF4-mediated transcription in T cells. *Nature* **490**, 543-546, doi:10.1038/nature11530 (2012).
65 Brass, A. L., Kehrli, E., Eisenbeis, C. F., Storb, U. & Singh, H. Pip, a lymphoid-restricted IRF, contains a regulatory domain that is important for autoinhibition and ternary complex formation with the Ets factor PU.1. *Genes & development* **10**, 2335-2347 (1996).
66 Escalante, C. R. *et al.* Crystallization and characterization of PU.1/IRF-4/DNA ternary complex. *Journal of structural biology* **139**, 55-59 (2002).
67 Ochiai, K. *et al.* Transcriptional regulation of germinal center B and plasma cell fates by dynamical control of IRF4. *Immunity* **38**, 918-929, doi:10.1016/j.immuni.2013.04.009 (2013).
68 Briseno, C. G. *et al.* Distinct Transcriptional Programs Control Cross-Priming in Classical and Monocyte-Derived Dendritic Cells. *Cell reports* **15**, 2462-2474, doi:10.1016/j.celrep.2016.05.025 (2016).
69 Eyster, C. A. *et al.* MARCH ubiquitin ligases alter the itinerary of clathrin-independent cargo from recycling to degradation. *Molecular biology of the cell* **22**, 3218-3230, doi:10.1091/mbc.E10-11-0874 (2011).
70 Grotzke, J. E. *et al.* Sec61 blockade by mycolactone inhibits antigen cross-presentation independently of endosome-to-cytosol export. *Proceedings of the National Academy of Sciences of the United States of America* **114**, E5910-e5919, doi:10.1073/pnas.1705242114 (2017).
71 De Angelis Rigotti, F. *et al.* MARCH9-mediated ubiquitination regulates MHC I export from the TGN. *Immunology and cell biology* **95**, 753-764, doi:10.1038/icb.2017.44 (2017).
72 Huang, L., Marvin, J. M., Tatsis, N. & Eisenlohr, L. C. Cutting Edge: Selective role of ubiquitin in MHC class I antigen presentation. *Journal of immunology* **186**, 1904-1908, doi:10.4049/jimmunol.1003411 (2011).
73 Masumi, A., Tamaoki, S., Wang, I. M., Ozato, K. & Komuro, K. IRF-8/ICSBP and IRF-1 cooperatively stimulate mouse IL-12 promoter activity in macrophages. *FEBS letters* **531**, 348-353 (2002).
74 Marquis, J. F. *et al.* Interferon regulatory factor 8 regulates pathways for antigen presentation in myeloid cells and during tuberculosis. *PLoS genetics* **7**, e1002097, doi:10.1371/journal.pgen.1002097 (2011).
75 Langlais, D., Barreiro, L. B. & Gros, P. The macrophage IRF8/IRF1 regulome is required for protection against infections and is associated with chronic inflammation. *The Journal of experimental medicine* **213**, 585-603, doi:10.1084/jem.20151764 (2016).
76 Rochman, Y. *et al.* TSLP signaling in CD4(+) T cells programs a pathogenic T helper 2 cell state. *Science signaling* **11**, doi:10.1126/scisignal.aam8858 (2018).
77 Macosko, E. Z. *et al.* Highly Parallel Genome-wide Expression Profiling of Individual Cells Using Nanoliter Droplets. *Cell* **161**, 1202-1214, doi:10.1016/j.cell.2015.05.002 (2015).

78 Chen, J., Bardes, E. E., Aronow, B. J. & Jegga, A. G. ToppGene Suite for gene list enrichment analysis and candidate gene prioritization. *Nucleic acids research* **37**, W305-311, doi:10.1093/nar/gkp427 (2009).

Acknowledgements:

We are grateful to the subjects who participated in this study. We would like to thank Dr Krista Dienger-Stambaugh, Cincinnati Children's Hospital Medical Center for technical help and Dr. Nathan Salomonis, for introduction to AltAnalyzer. We acknowledge the use of the IRIDIS High Performance Computing Facility and Flow Cytometry Core Facilities, together with support services at the University of Southampton.

Author Contributions:

MEP and HS: intellectually conceived and wrote the manuscript,
MEP, MAJ, SS, KC, ZW: Biological experiments and flow cytometry, processing of RNA and chromatin
MEP, JW, VC,TW: analysis and meta-analysis of bulk RNA-seq data
MEP, JR, MP, XC, MW: analysis of ChIP-seq data
MAJ, PS, MW: reviewing of the manuscript
MEP, PS, MRZ, JW, AV, JD, MacA, SS: processing cells for scRNA-seq, pre-processing and analysis of scRNA-seq data
SS,LN,GW, MEP: CRISPR-Cas9 editing

Competing Interests:

The Authors declare no conflict of interest

Materials and correspondence:

Dr. Marta E Polak e-mail: m.e.polak@soton.ac.uk

Prof. Harinder Singh e-mail: harinder@pitt.edu

Figure Legends

Figure 1. System for analysing human LCs and control of antigen cross-presentation

a) Schematic depicting isolation of primary human LCs. Split healthy skin was treated with dispase for 20h to dissociate epidermis. Steady-state LCs were isolated from the epidermis by digestion with liberase TM or migrated from the epidermal sheets for 48h in cell culture medium and stimulated with TNF (24h) to induce their activation.
b) Flow cytometry assessment of steady-state and migrated LC. LCs were enumerated as CD207/CD1a/HLA-DR high cells. A representative example of n>5 independent donors.
c) Flow cytometry assessment of activation markers expressed by steady-state and migrated LC. Co-stimulatory molecules critical for T cell activation during antigen presentation (CD70, CD86 and CD40) were analysed in CD207/CD1a/HLA-DR high cells. A representative example of n>5 independent donors.
d) IFN-γ secretion by an EBV-specific CD8 T cell line stimulated with antigen presenting LCs in the context of MHC I HLA-A2. Steady-state or migrated LCs were pulsed with 30 amino acid peptide containing EBV epitope (dark grey). Pulsed or unpulsed (light gray) LCs were stimulated with TNF and then assayed for IFN-γ secretion. ELISpot assay, n=5

independent experiments in triplicate, paired t-test, box and whiskers show min and max value, line at median.

e) IFN-γ secretion by EBV-specific CD8 T cell line stimulated by migrated LCs pulsed as in panel 1d. IFN-γ secretion was measured with (black) or without (grey) TNF stimulation. ELISpot assay, n=5 independent experiments in triplicate, paired t-test, box and whiskers show min and max value, line at median.

Figure 2. Transcriptional programming of migrated human LCs

a) Dominant biological processes and pathways enriched in genes expressed at varying levels in steady state migrated LCs. Gene ontology analysis for each expression level (Fragments Per Kilobase of transcript per Million mapped reads, FPKM) interval determined by RNA-seq was performed using ToppGene on-line tool[78]. Line denotes median value in the interval. Top unique Biological processes are shown for each interval, significance denoted by FDR (Benjamini- Hochberg) corrected p-value is shown. The x-axis shows consecutive cut-offs for each interval in gene expression levels.

b) Overlaps between reported cross-presentation (373 genes) and antigen processing (212 genes) signatures, and genes expressed in migrated LC >10 FPKM.

c) Intracellular expression of SQSTM1 and TRIM21 measured by flow cytometry. Steady-state (blue) and migrated (red) LCs. Representative histograms followed by quantitative analysis n=4 independent donors, unpaired t-test, line denotes median value.

d) TNF stimulation (24h) of human LCs induces genes involved in antigen trafficking (red), processing (purple) and cross-presentation (blue). Expression levels of 3 biological replicates (TMM normalised gene expression levels, scaled in rows).

e) Enrichment of immune activation genes upregulated during a time course of TNF stimulation: left: early induced genes, peak expression at 2h, Cluster 3, right: late induced genes, peak expression at 24h. Median of 3 biological replicates, normalised expression levels. Stars denote genes belonging to antigen presentation in class I, MSigBD, Broad Institute.

Figure 3. scRNA-seq analysis of migrated human LCs

a) UMAP plot of 950 migrated LCs (ScanPy, Leiden r = 0.2, n_pcs=4, n_neighbours =10, 2464 highly variable genes (min_mean=0.0125, max_mean=6, min_disp=0.6) defines 3 major clusters of LCs .

b) Pseudotrajectory analysis of the transcriptomes of 950 migrated LCs (ScanPy, diffmap: Leiden r = 0.2, n_pcs=4, n_neighbours =10). Cells are color coded for clusters as in panel a.

c) Gene ontology analysis for marker genes (n=100) representative of indicated cluster, performed using ToppGene. –log(10) Benjamini Hochberg corrected p values are shown for cluster-specific processes.

d) Barplots displaying frequency and amplitude expression of indicated gene transcripts. Bars are color coded for cells as in panel **a**. Representative uniformly expressed genes characteristic of LCs (top panel), genes involved in antigen presentation and processing (middle panels) and genes functioning in oxidative phosphorylation (bottom panel) are displayed. Each bar shows CPTT (counts per ten thousand) normalised expression level of indicated transcript in a given LC.

Figure 4. Chromatin landscape of migrated LCs enriches for EICE, AICE and ISRE motifs

Human steady state migrated LCs were subjected to whole genome chromatin profiling of H3K4me3 and H3K27Ac.

a) Proportion of DEG with H3K27Ac mark at 2h in clusters of co-expressed genes up-regulated early (2h, clusters 3) and late (24h, cluster 2) following stimulation with TNF. Changes in H3K27Ac acetylation were calculated using MANorm algorithm embedded in BioWardrobe tool. Genes were filtered to include unique common entry across the biological replicates (consensus value from n=3 independent donors). Genes with detected changes in acetylation were intersected with DEGs identified by EdgeR analysis.
b) UCSC genome browser tracks of H3K27Ac mark changes in human migrated LCs over the timecourse of stimulation with TNF. Early ubiquitin C, UBC (top) and CD40 (bottom) and late sequestosome SQSTM1 (top) and TRIM22 (bottom) induced genes. Red rectangle denotes promoter site, a representative example.
c) Promoter sites of genes acetylated at H3K27 in migrated human LCs are enriched in IRF-binding composite DNA elements. EICE is the top human motif enriched at steady state LCs (HOMER de novo motif detection analysis, median –logp value shown).
d) Peaks H3K4Me3 and H3K27Ac T0 datasets were scanned for ISRE/AICE/EICE binding motifs. 1193 consensus genes (present in all 3 biological replicates with both chromatin marks) were identified. Biological processes enriched in those genes were detected using ToppGene based on FDR corrected p-values for GO categories).

Figure 5. Human LCs upregulate expression of IRF4 upon migration but lack IRF8

a) IRF4, but not IRF8 protein expression is upregulated in BATF3 positive LC during migration from the epidermis. A representative FACS analysis of 3-5 independent donors, gates set using isotype controls for each antibody (nuclear staining for IRF4, IRF8 and BATF3).
b) IRF4 protein expression in steady state vs migrated LCs. $IRF4^+$ LCs (%) as measured by flow cytometry, median ± range, n=4, 3 paired samples from independent donors, unpaired t-test, box and whiskers show min and max value, line at median.
c) Transcript levels of key transcription factors in migrated LCs before and after TNF stimulation (2h, 24h). FPKM values, median $\pm$ range of 3 biological donors shown.
d) Expression of IRF4 and BATF3 in response to TNF signalling (24h). Representative graphs of 5 independent donors, gates set using isotype controls for each antibody (Nuclear staining for IRF4, IRF8 and BATF3).

Figure 6. IRF4-mediated transcriptional programming of human LCs

Knock down (KD) of IRF4 using CRISPR-Cas9 editing. An IRF4 guide - CAS9 complexes were introduced by nucleofection into migrated LCs. Indicated analyses were performed 48 hours after nucleofection.

a) Intranuclear expression levels of IRF in CRISPR-Cas9 edited (orange) and control (blue) migrated LCs measured using flow cytometry in CD207+ CD1a+ live LCs. A representative example of n=3 independent donors.
b) Quantification of the intranuclear expression levels of IRF4 in CRISPR-Cas9 edited (orange) and control (blue) migrated LCs. Mean fluorescence intensity (MFI) of IRF4 expressing CD207+ CD1a+ live LCs shown, n=3 independent donors, paired t-test, box and whiskers show min and max value, line at median.

c) scRNA-seq analysis of WT and IRF4 KD migrated LCs. UMAP plot of 1484 LCs (WT:617 cells, blue, KD, 867 cells, orange). (Filtering setting gene count 500-10000 per cell, expression of mitochondrial genes <0.2, Leiden r= 0.2).

d) GO processes and pathways differentially enriched in control LC (WT, left) versus IRF4 CRISPR-Cas9 edited LCs (IRF4 KD, right). DEG analysis was performed using Single TK package, scDiffExlimma algorithm, scnorm data, FDR corrected p value used as a significance measure. Gene ontology enrichment: ToppGene tool, Biological Processes and Molecular Function.

e) Barplots of genes expressed at higher levels in WT LCs. Each bar shows CPTT normalised expression level of indicated gene in a given WT LC cell (blue) or IRF4 CRISPR-Cas9 edited LC (orange). IRF4 plus top 5 genes by FDR corrected p value and 5 genes representative for biological processes enriched in WT are displayed.

f) Barplots of genes expressed at higher levels in IRF4 KD LCs. Each bar shows CPTT normalised expression level of indicated gene in a given WT LC cell (blue) or IRF4 CRISPR-Cas9 edited LC (orange). Top 5 genes by FDR corrected p value and 5 genes representative for biological processes enriched in KO are displayed.

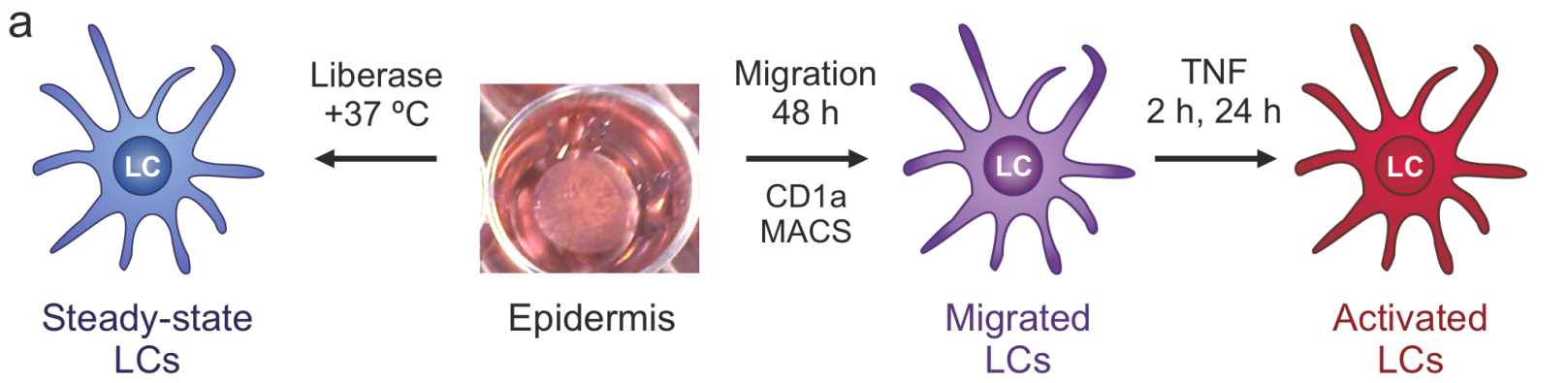
a
LC
Liberase
+37 ºC
Epidermis
Migration
48 h
CD1a
MACS
LC
TNF
2 h, 24 h
LC
Steady-state
LCs
Migrated
LCs
Activated
LCs

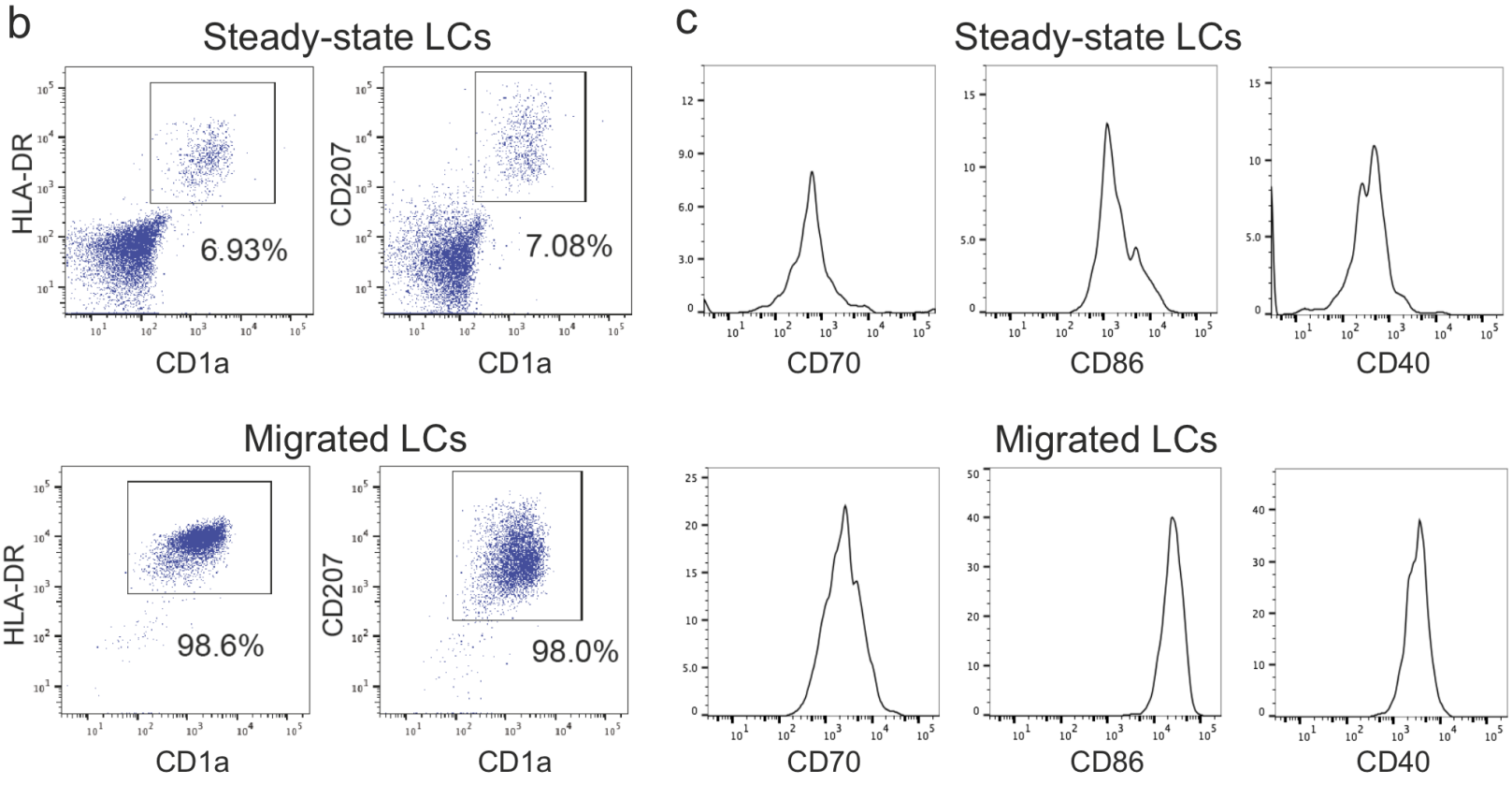
b
Steady-state LCs
HLA-DR
6.93%
CD1a
CD207
7.08%
CD1a
Migrated LCs
HLA-DR
98.6%
CD1a
CD207
98.0%
CD1a
c
Steady-state LCs
CD70
CD86
CD40
Migrated LCs
CD70
CD86
CD40

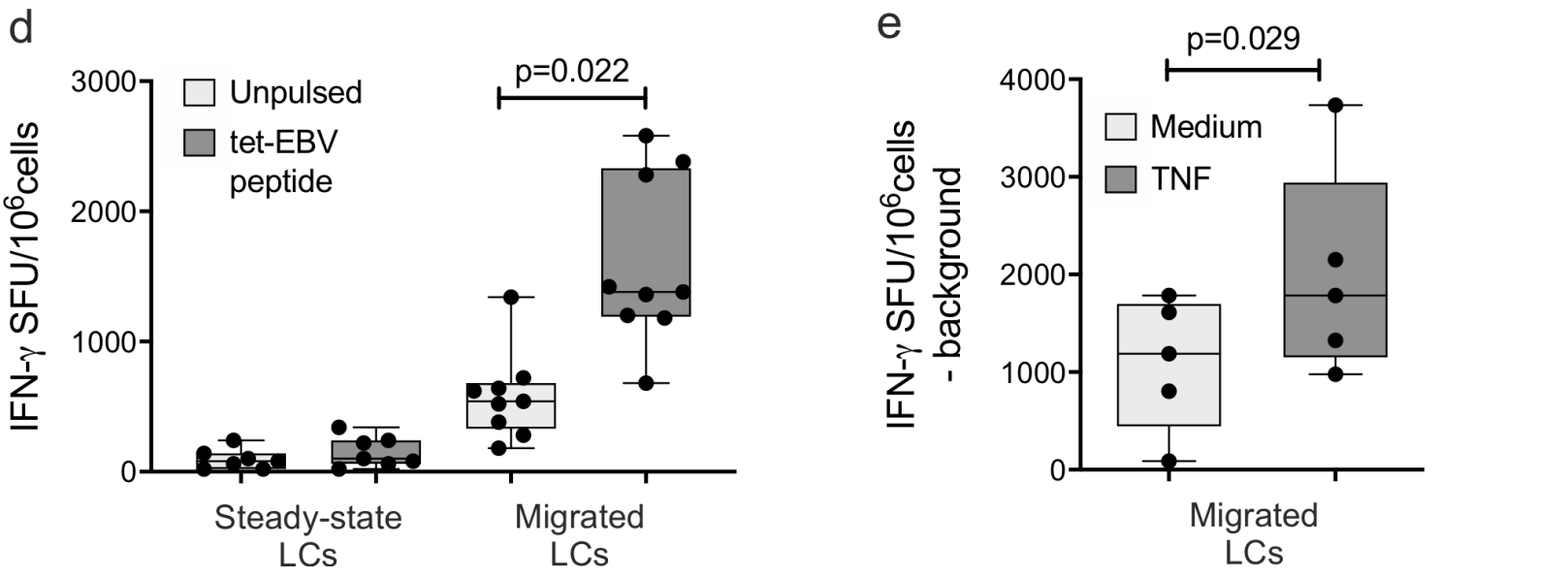
d
IFN-γ SFU/10^6cells
3000
2000
1000
0
Unpulsed
tet-EBV
peptide
p=0.022
Steady-state
LCs
Migrated
LCs
e
IFN-γ SFU/10^6cells
- background
4000
3000
2000
1000
0
p=0.029
Medium
TNF
Migrated
LCs

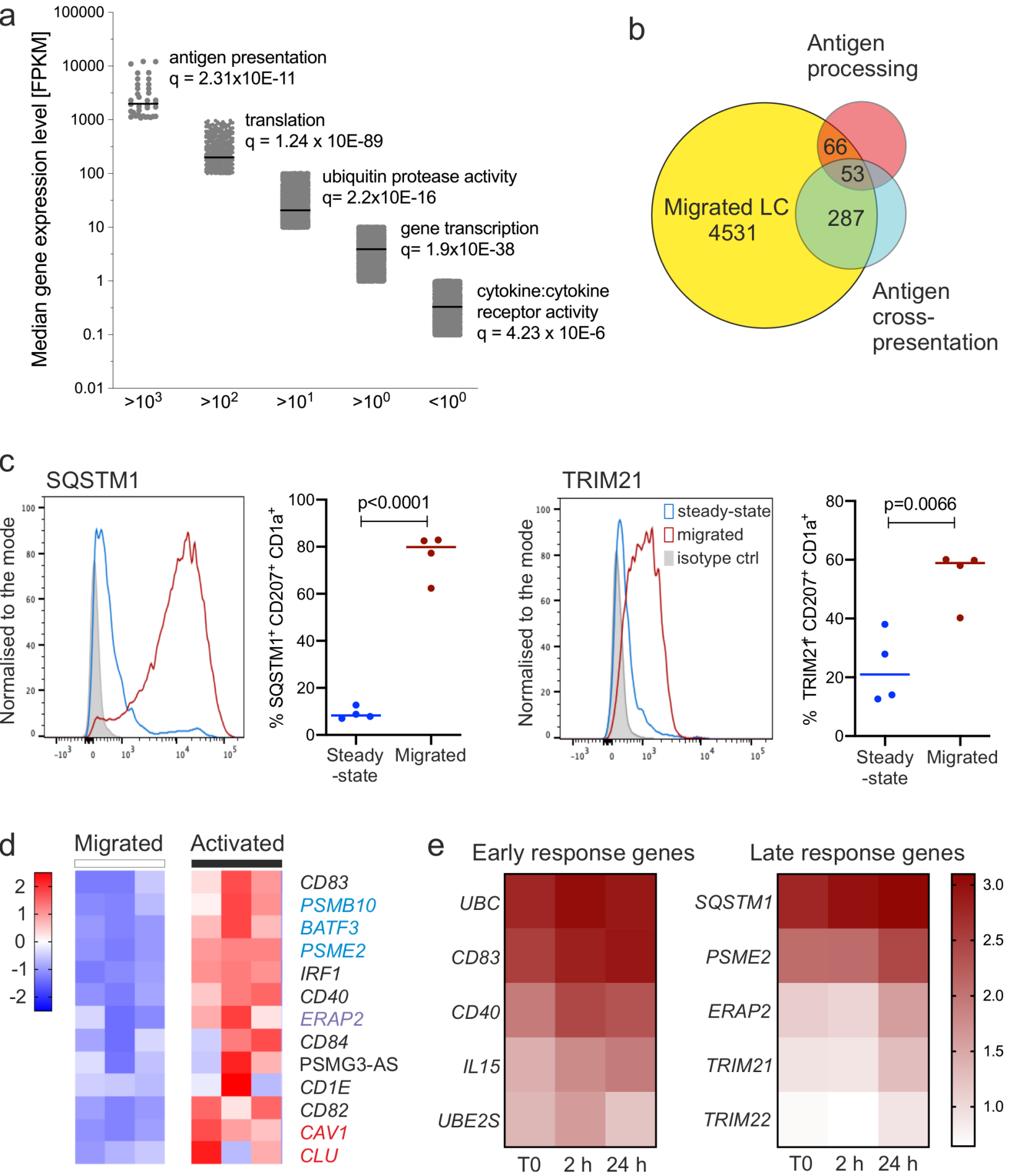
a
Median gene expression level [FPKM]
100000
10000
1000
100
10
1
0.1
0.01
antigen presentation
q = 2.31x10E-11
translation
q = 1.24 x 10E-89
ubiquitin protease activity
q= 2.2x10E-16
gene transcription
q= 1.9x10E-38
cytokine:cytokine
receptor activity
q = 4.23 x 10E-6
>10^3
>10^2
>10^1
>10^0
<10^0
b
Antigen
processing
66
53
Migrated LC
4531
287
Antigen
cross-
presentation
c
SQSTM1
Normalised to the mode
% SQSTM1+ CD207+ CD1a+
p<0.0001
Steady
-state
Migrated
TRIM21
steady-state
migrated
isotype ctrl
% TRIM21+ CD207+ CD1a+
p=0.0066
d
Migrated
Activated
CD83
PSMB10
BATF3
PSME2
IRF1
CD40
ERAP2
CD84
PSMG3-AS
CD1E
CD82
CAV1
CLU
e
Early response genes
Late response genes
UBC
CD83
CD40
IL15
UBE2S
SQSTM1
PSME2
ERAP2
TRIM21
TRIM22
T0
2 h
24 h

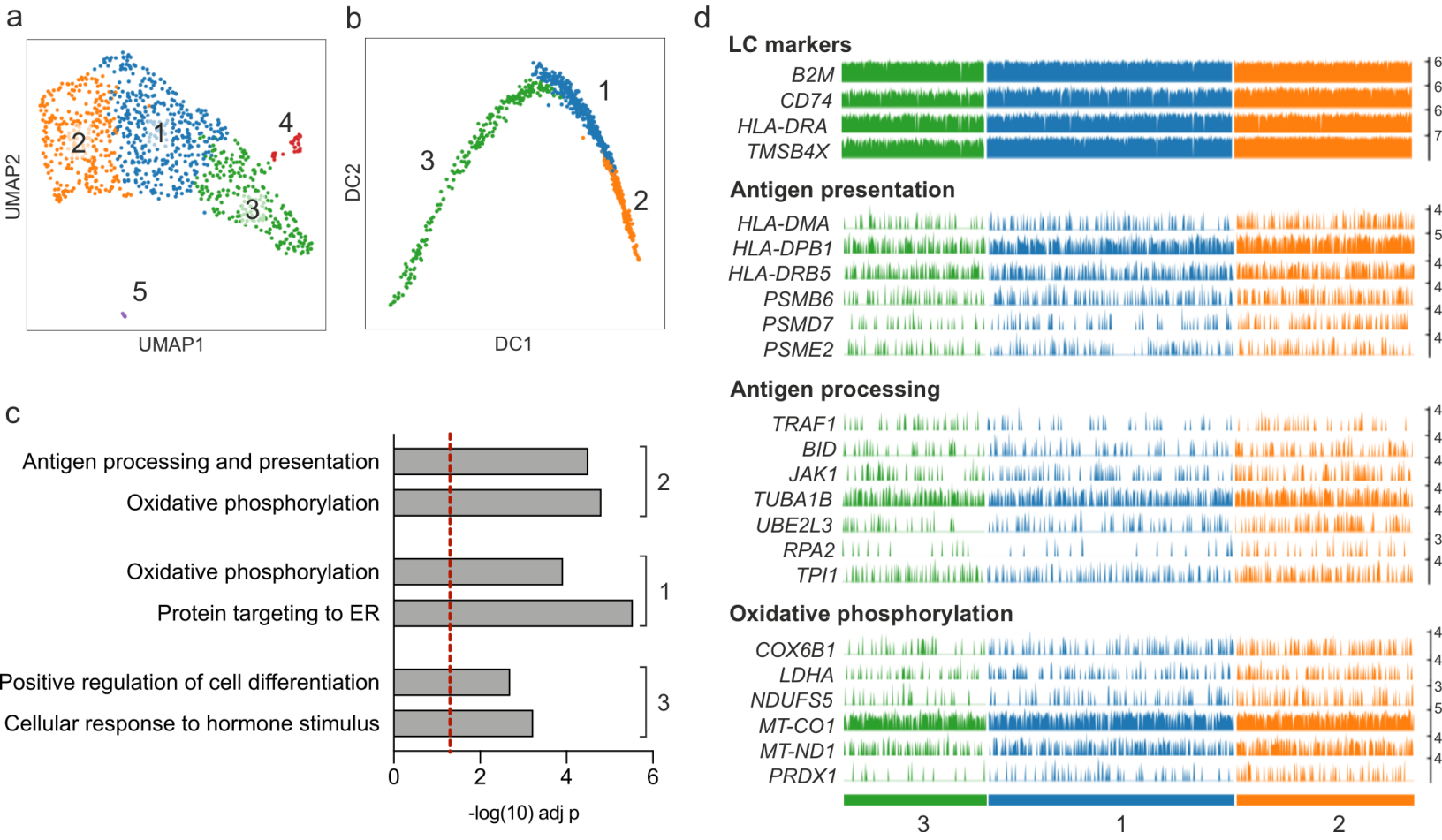
a
UMAP2
UMAP1
1
2
3
4
5
b
DC2
DC1
1
2
3
c
Antigen processing and presentation
Oxidative phosphorylation
Oxidative phosphorylation
Protein targeting to ER
Positive regulation of cell differentiation
Cellular response to hormone stimulus
2
1
3
0
2
4
6
-log(10) adj p
d
LC markers
B2M
CD74
HLA-DRA
TMSB4X
Antigen presentation
HLA-DMA
HLA-DPB1
HLA-DRB5
PSMB6
PSMD7
PSME2
Antigen processing
TRAF1
BID
JAK1
TUBA1B
UBE2L3
RPA2
TPI1
Oxidative phosphorylation
COX6B1
LDHA
NDUFS5
MT-CO1
MT-ND1
PRDX1
3
1
2

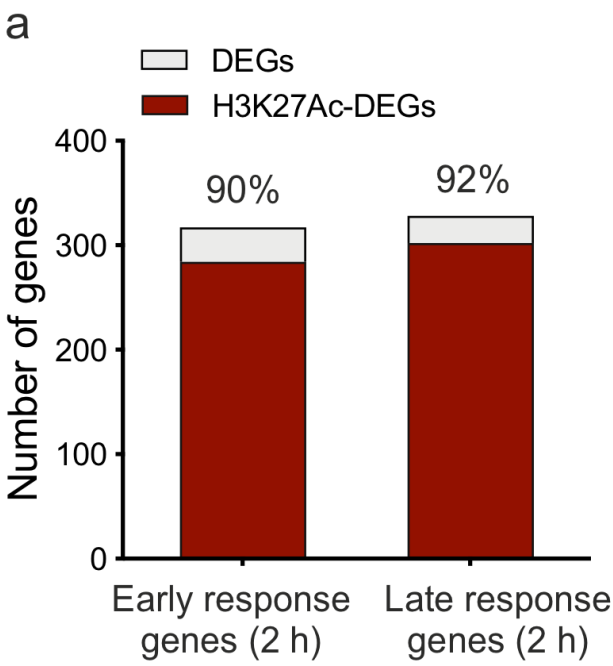
a
DEGs
H3K27Ac-DEGs
Number of genes
400
300
200
100
0
90%
92%
Early response genes (2 h)
Late response genes (2 h)

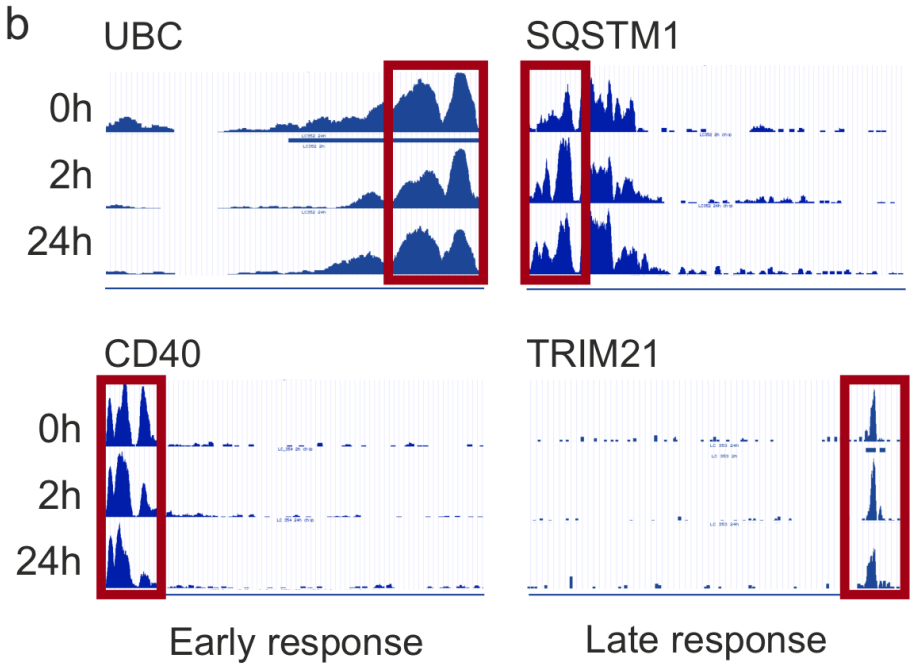
b
UBC
SQSTM1
0h
2h
24h
CD40
TRIM21
0h
2h
24h
Early response
Late response

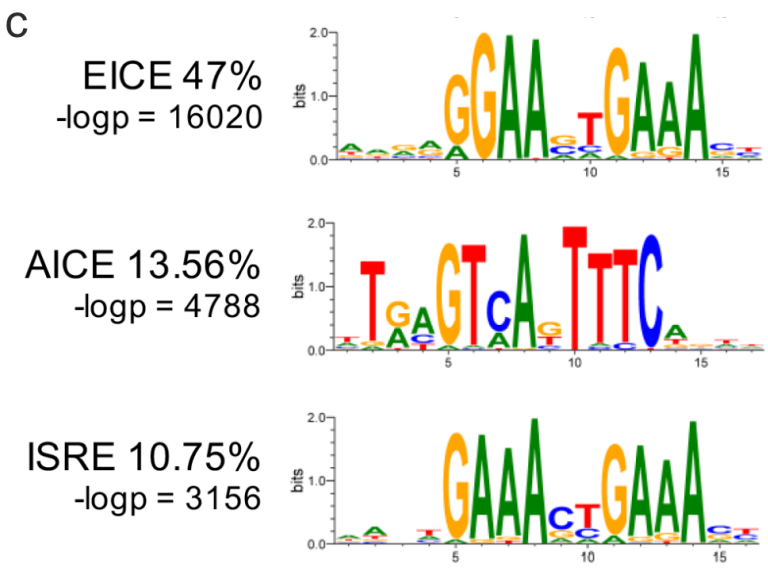
c
EICE 47%
-logp = 16020
AICE 13.56%
-logp = 4788
ISRE 10.75%
-logp = 3156
bits

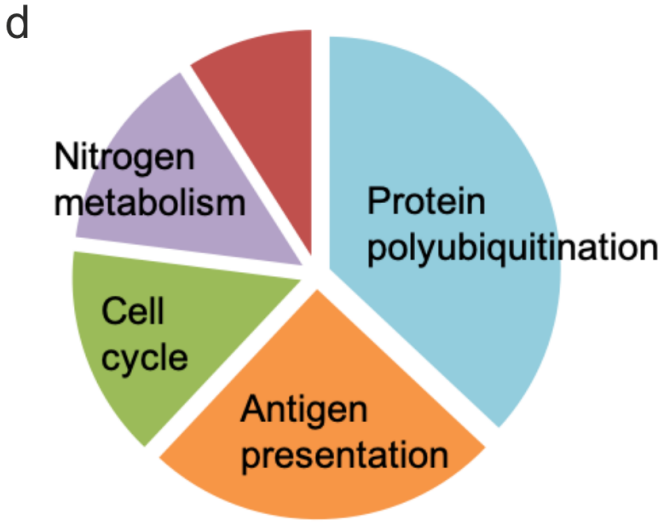
d
Nitrogen metabolism
Protein polyubiquitination
Cell cycle
Antigen presentation

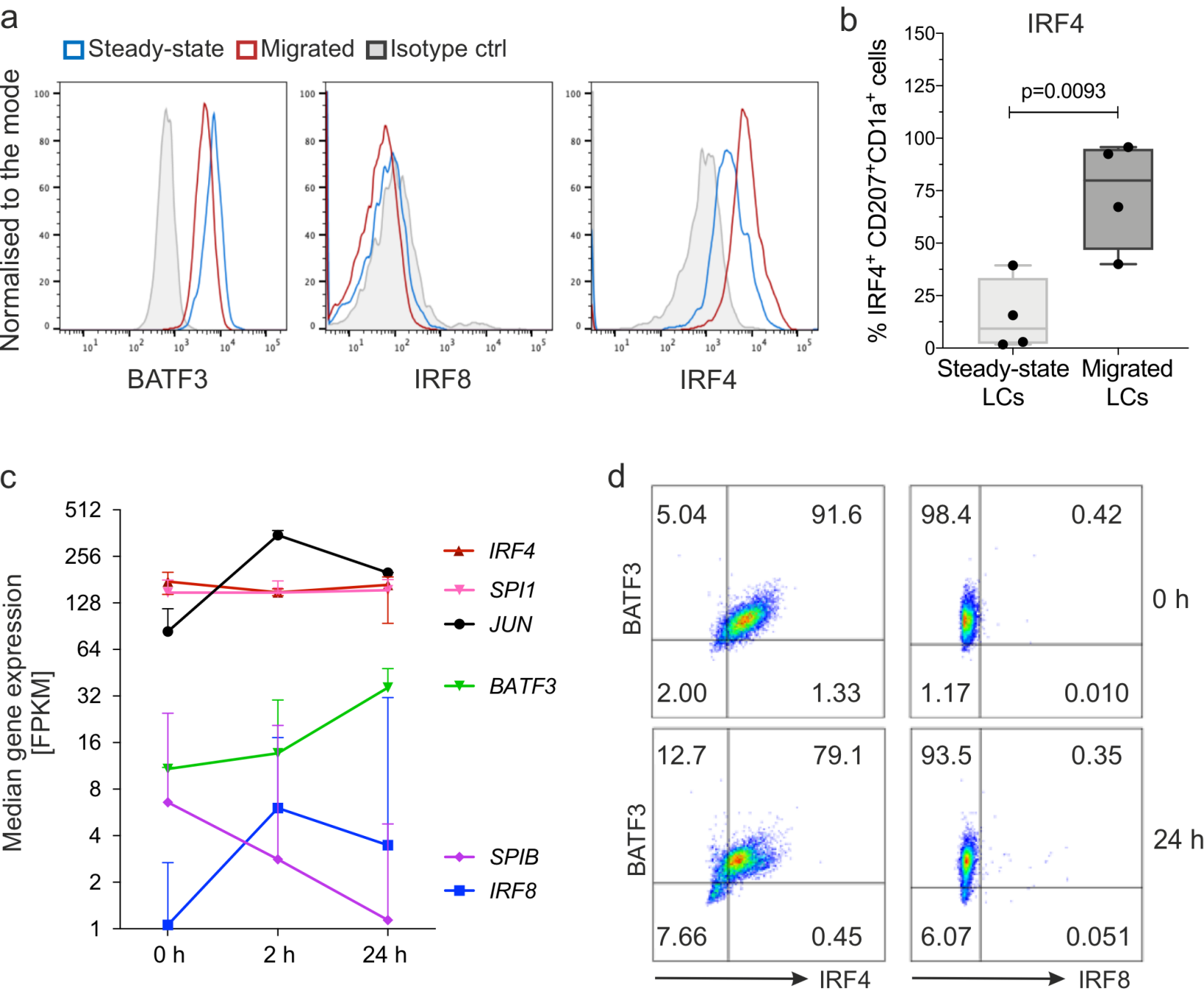
a
Steady-state
Migrated
Isotype ctrl
Normalised to the mode
BATF3
IRF8
IRF4
b
IRF4
p=0.0093
% IRF4+ CD207+CD1a+ cells
Steady-state LCs
Migrated LCs
c
Median gene expression [FPKM]
IRF4
SPI1
JUN
BATF3
SPIB
IRF8
0 h
2 h
24 h
d
BATF3
IRF4
IRF8
0 h
24 h
5.04
91.6
2.00
1.33
98.4
0.42
1.17
0.010
12.7
79.1
7.66
0.45
93.5
0.35
6.07
0.051

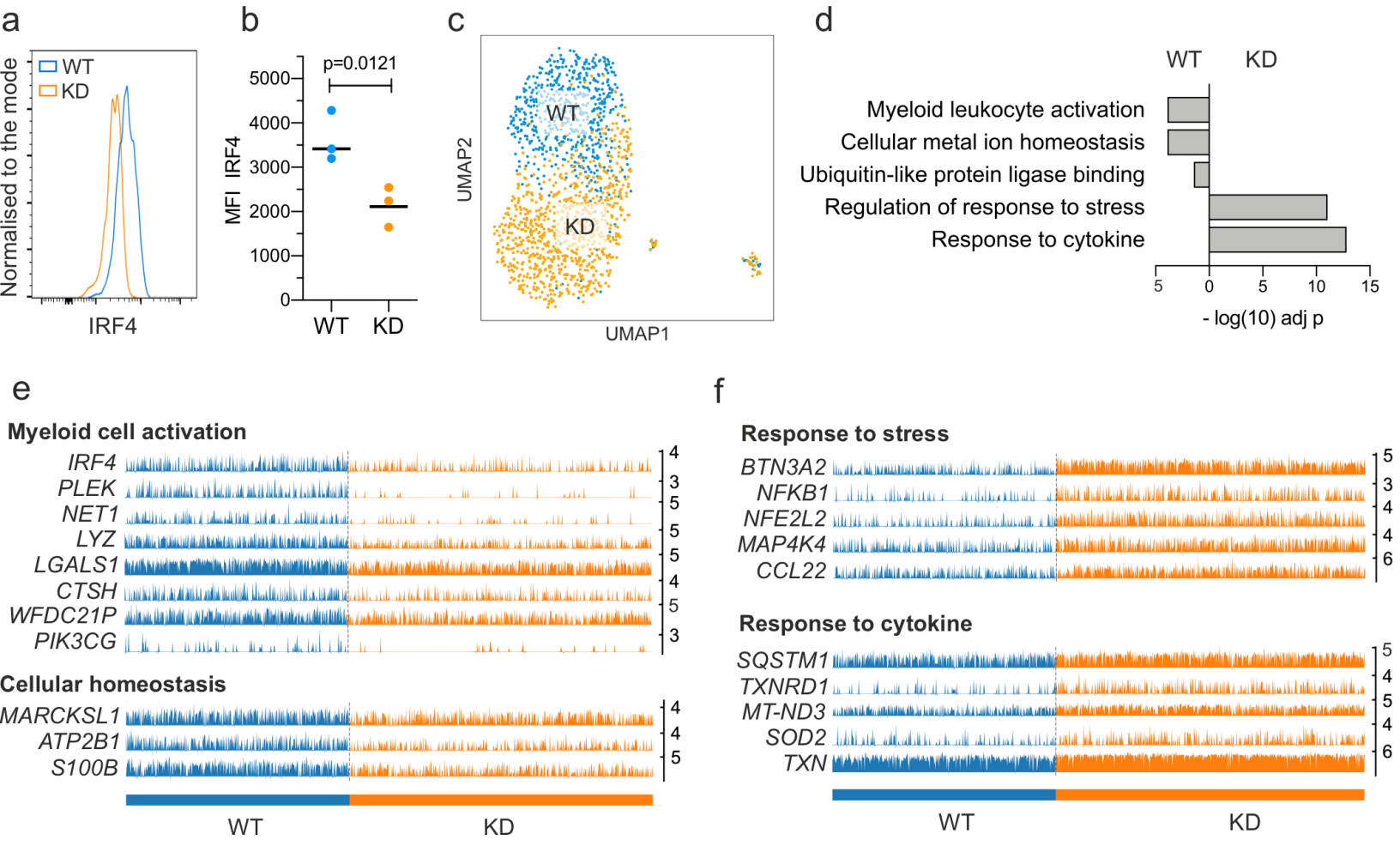
a
WT
KD
Normalised to the mode
IRF4
b
p=0.0121
MFI IRF4
5000
4000
3000
2000
1000
0
WT
KD
c
WT
KD
UMAP2
UMAP1
d
WT
KD
Myeloid leukocyte activation
Cellular metal ion homeostasis
Ubiquitin-like protein ligase binding
Regulation of response to stress
Response to cytokine
5
0
5
10
15
- log(10) adj p
e
Myeloid cell activation
IRF4
PLEK
NET1
LYZ
LGALS1
CTSH
WFDC21P
PIK3CG
Cellular homeostasis
MARCKSL1
ATP2B1
S100B
WT
KD
f
Response to stress
BTN3A2
NFKB1
NFE2L2
MAP4K4
CCL22
Response to cytokine
SQSTM1
TXNRD1
MT-ND3
SOD2
TXN
WT
KD